J. metamorphic Geol., 2002, **20,** 87–98

Long-term thermal consequences of the redistribution of heat-producing elements associated with large-scale granitic complexes

M. SANDIFORD,[1] S. MCLAREN[2] AND N. NEUMANN[2]
[1]*School of Earth Sciences, University of Melbourne, Victoria 3010, Australia (m.sandiford@earthsci.unimelb.edu.au)*
[2]*Department of Geology and Geophysics, University of Adelaide, South Australia 5005, Australia*

ABSTRACT Crustal thermal regimes are sensitive to both the amount and distribution of heat producing elements (HPEs). Since a significant proportion of the crustal complement of HPEs is contained within granites, granite generation and emplacement should lead to significant long-term changes in the thermal structure of the crust. Using HPE concentrations appropriate to representative Australian Proterozoic granites we show that granite segregation leads to changes in the temperature field of the crust of up to *c.* 50 °C, producing long-term cooling in the source regions and heating at emplacement levels, relative to the pre-granite conductive thermal regime. Because of the intimate connection between thermal regime and lithospheric strength, granite-assisted redistribution of HPEs is likely to be fundamental to cratonisation.

Key words: granitic complexes; heat producing elements; Sybella Batholith.

INTRODUCTION

Granites are typically enriched in heat producing elements (HPEs) compared with bulk crust (e.g. Haenel *et al.*, 1988; Fowler, 1990). Therefore, they play an important role in shaping the geochemical and thermal structure of the continental crust, with the more felsic mid to upper crust enriched in HPEs relative to the more mafic lower crust. In terms of HPE distributions, a differentiated crust consisting of granitic upper crust and a depleted lower crust can be contrasted with an undifferentiated crust in which the HPEs are more uniformly distributed (Fig. 1a). The potential significance of the HPE differentiation associated with the generation of a granitic upper crust can be illustrated by comparing the thermal structure of this differentiated crust with its undifferentiated counterpart, using characteristic heat production values (Fig. 1). Heat production in typical continental crust is estimated to contribute about half of the average continental surface heat flow of 65 mWm^{-2} (Pollack *et al.*, 1993) suggesting a bulk crustal heat production rate of *c.* 1 μWm^{-3} (McLennan & Taylor, 1996). In comparison, the heat production in 'average' granite is *c.* 2.5 μWm^{-3} (e.g. Haenel *et al.*, 1988; Fowler, 1990).

Following Sandiford & McLaren (2001), for one-dimensional models with constant mantle heat flow, q_m, the contribution of crustal heat production to the temperature at the Moho can be expressed quite simply as (Fig. 2):

$$T'_{q_c} = \frac{q_c h}{k} \tag{1}$$

where q_c is the vertically integrated heat production (in a column of unit width), h is the effective depth of the heat production, and k is thermal conductivity. In terms of the distribution of HPEs, crustal differentiation changes the effective depth by an amount Δh. For constant q_c, the long-term change in temperature at the Moho resulting from differentiation can be related to Δh:

$$\Delta T'_{q_c} = \frac{q_c \Delta h}{k} \tag{2}$$

The potential significance of redistribution can be illustrated by the following simplified example. In a 35-km thick crust with uniform heat production of 1 μWm^{-3}, $q_c = 35$ mWm^{-2} and $h = 17.5$ km. In a differentiated crust, the same contribution to surface heat flow will be provided by a 10-km thick granite layer with heat production of 3.5 μWm^{-3}. For the extreme case where differentiation has left a completely depleted lower crust, the mean depth of the HPE distribution is half the thickness of the granite layer (i.e. 5 km), equating to a reduction in h of 12.5 km. For a thermal conductivity of 2.5 $Wm^{-1}\,K^{-1}$, the

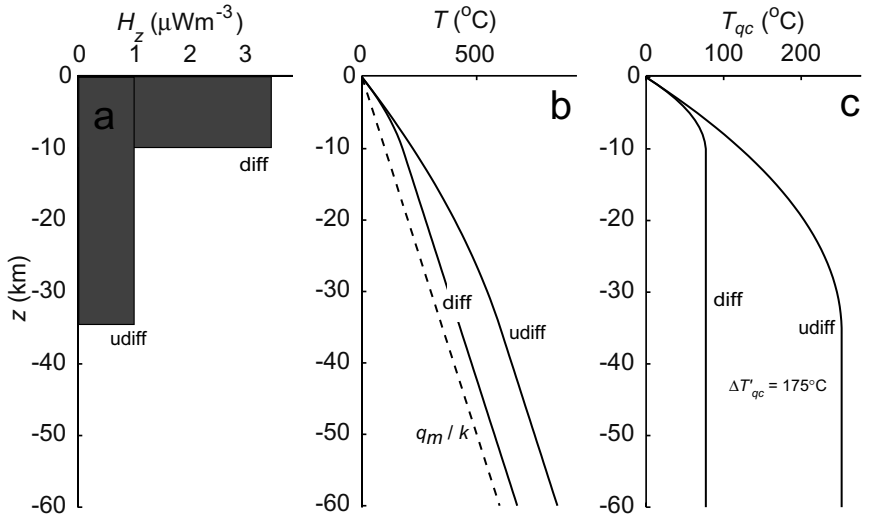

Fig. 1. Illustration of the effects of crustal differentiation on thermal regime. (a) shows HPE distributions in an undifferentiated lithospheric column (*udiff*) and a differentiated (*diff*) column. Each column contains the same vertically integrated heat production, q_c, and therefore contributes the same amount to the surface heat flow. (b) Geotherms corresponding to the HPE distributions *udiff* and *diff*, respectively. The dashed line represents the contribution due to mantle heat flow and has slope q_m/k where q_m is the mantle heat flow, and k is the thermal conductivity. (c) plots of the crustal contribution to the geotherm, T_{qc}, show that HPE differentiation from a distribution like *udiff* to a distribution like *diff* would result in a 175 °C reduction in the conductive Moho temperature. Despite this enormous difference in Moho temperature the surface heat flow remains unaffected, emphasising the fact that the distribution of the HPEs is just as important as the total amount of HPEs in determining geothermal structure.

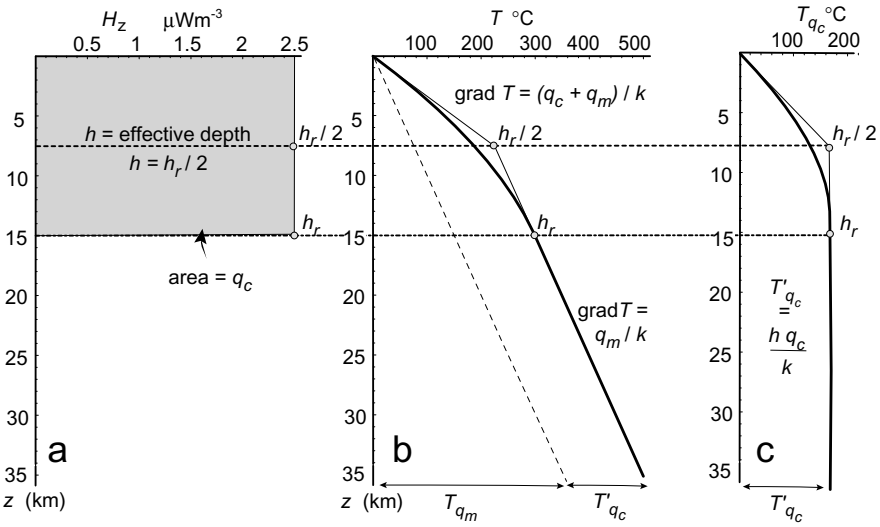

Fig. 2. Illustration highlighting the connection between the effective depth of the crustal heat production h, the vertically integrated complement of HPEs, q_c, and the perturbation of the geotherm due to the heat production, T_{qc}. The maximum value, T'_{qc}, occurs at the base of the heat producing layer and is given by $h\, q_c/k$. For a layer of uniform heat production of thickness h, $h = h/2$.

differentiation equates with a conductively equilibrated Moho temperature reduction of 175 °C.

Although the simple calculations summarised here and in Fig. 1 highlight the potential role played by granitic magmatism in controlling the long-term thermal structure of the lithosphere, their significance is obscured by the knowledge that crustal differentiation is a complex, prolonged process often involving many cycles of magmatism, which not only redistribute HPEs through crustal melt generation and migration but also add HPEs to the crust through magmatic additions from the mantle. Nevertheless, it is clear from the calculations outlined above that the development of large granitic complexes must have fundamental, long-term consequences for the thermal structure of the lithosphere. This paper provides a quantitative assessment of the long-term thermal consequences of the generation and emplacement of large HPE-bearing granitic complexes. We begin with an assessment of the HPE fluxes associated with large granitic complexes in the Australian Proterozoic, which are known to contain elevated concentrations of U, Th and K and other incompatible elements (e.g. Wyborn *et al.*, 1992). The impact of the redistribution of HPEs has important

implications for the thermal evolution of Australian Proterozoic metamorphic terranes, as discussed elsewhere by Sandiford & Hand (1998), Sandiford *et al*., (1998), McLaren *et al*., (1999) and McLaren & Sandiford (2001).

EXAMPLES OF HPE-RICH GRANITES FROM PROTEROZOIC AUSTRALIA

The Australian Proterozoic provides numerous examples where significant redistribution of the HPEs must have accompanied granite emplacement. As documented by Sandiford & Hand (1998), McLaren *et al*., (1999), McLaren & Sandiford (2001) and Neumann *et al*., (2000), the total abundance of HPEs contained within granites in Australian Proterozoic terranes is constrained by both regional geochemical datasets and present day surface heat flow data. In this section we briefly summarise these results in order to assess the concentration of HPEs contained within individual large-scale granite complexes. This provides a constraint on the total flux of HPEs associated with the production of large-scale granite complexes.

The *c.* 120 heat flow determinations from Australia (Cull, 1982) point to a three-fold subdivision of the Australian heat flow field more or less coinciding with Archean, Proterozoic and Phanerozoic terranes, respectively (Fig. 3). In the Proterozoic Central Shield Province (Sass & Lachenbruch, 1979), the heat flow averages about 85 mWm^{-2} (Fig. 4), more than 30 mWm^{-2} higher than expected on the basis of measurements from similarly aged terranes elsewhere in the world (e.g. Morgan, 1984; Chapman & Furlong, 1977). The existence of thick, cold mantle lithosphere beneath much of the Central Shield Province (e.g. Collins, 1991; Van der Hilst *et al*., 1994; Zielhaus & Van der Hilst, 1996), together with the absence of recent tectonic or magmatic activity, points towards low mantle heat flow in this region. This in turn suggests that the high heat flows are more likely to reflect elevated HPE concentrations (Sandiford & Hand, 1998; Neumann *et al*., 2000).

In terms of contemporary heat flow measurements, the best constrained part of this province is South Australia, where 22 measurements define an elevated heat flow zone at least 250 km wide. Eleven determinations within the anomalous zone average 92 mWm^{-2} (Neumann *et al*., 2000), compared with an average of *c.* 50 mWm^{-2} to the west of this zone. Regional geochemical datasets show that the heat flow anomaly is explicable in terms of elevated upper crust HPE concentrations. The characteristic upper crustal heat production, defined by a regional geochemical dataset comprising some 2550 bulk rock analyses, increases from *c.* 2.8 μWm^{-3} outside the anomalous zone, to *c.* 6 μWm^{-3} in the anomalous zone, and as high as 10 μWm^{-3} for select areas such as the Mount Painter province in the northern Flinders Ranges (Sandiford *et al*., 1998). Within this region Mesoproterozoic granites host the major proportion of the near surface HPE complement with the highest heat production value of 62 μWm^{-3} from the Yerila Granite. Given that 'average' granite heat production is approximately 2.5 μWm^{-3} (e.g. Haenel *et al*., 1988), the South Australian values are extraordinary and suggest the possibility of secondary enrichment due to hydrothermal alteration. While this is undoubtedly the case in some instances, an average Th/U ratio of

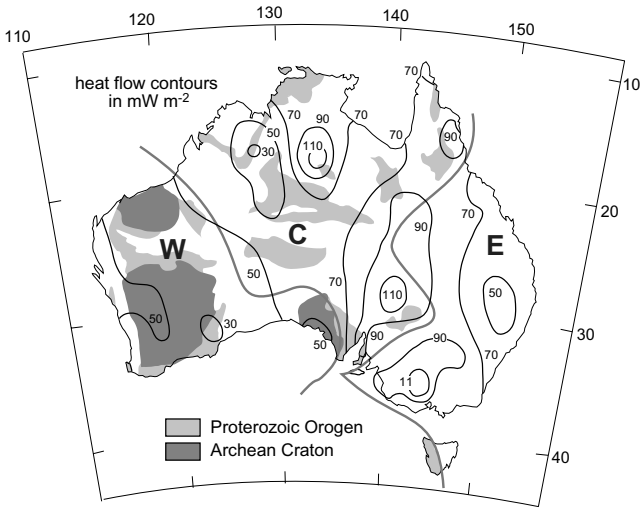

Fig. 3. Heat flow map of Australia modified from Cull (1982) showing the three-fold subdivision proposed by Sass & Lachenbruch (1979). Note the coincidence between elevated heat flow values of the Central Shield Province and the occurrence of Proterozoic terranes.

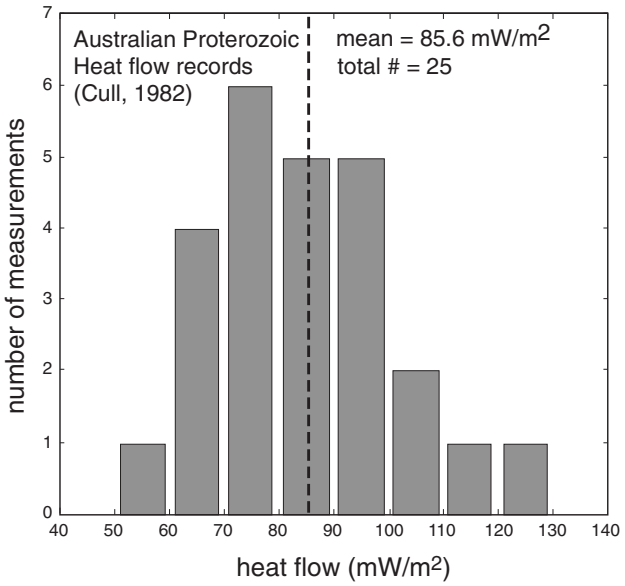

Fig. 4. Summary of heat flow data from Australian Proterozoic terranes (data from Cull, 1982).

approximately 4 (Neumann *et al.*, 2000), combined with evidence for regionally elevated heat flow, imply that: (1) the near surface enrichment reflects primary magmatic processes, and (2) the bulk crust is enriched in HPEs, perhaps by as much as a factor of 2.

A similar geochemical scenario occurs in the Mount Isa province in Queensland, and the Pine Creek and the Northern Arunta Inliers in the Northern Territory (Table 1). In each case, granites with elevated heat production rates comprise significant proportions of the terrane (McLaren *et al.*, 1999; Sandiford & Hand, 1998). For example, the Sybella Batholith near Mt Isa forms a sill which outcrops over more than 1200 km^2, with an average modern day heat production rate of 5.1 μWm^{-3} (McLaren *et al.*, 1999). The preserved remnants of the sill are about 1.5 km thick (McCready, 1997) with the original thickness likely to have been closer to 3 km. At intrusion at *c.* 1660 Ma (Connors & Page, 1995), the mean heat production was *c.* 6.9 μWm^{-3} (Table 1) implying it then hosted a complement of HPEs equivalent to at least 10 mWm^{-2} (if it were no thicker than 1.5 km) and probably closer to 20 mWm^{-2}. Given that the complement of HPEs in average continental crust is estimated to be *c.* 30 mWm^{-2} (McLennan & Taylor, 1996), it seems likely that the generation of the Sybella Batholith must have effected the redistribution of a significant fraction of the crustal complement of HPEs. In the Eastern fold belt of the Mt Isa block, similar-scale bodies with significantly higher heat production rates include the Williams and Naraku Batholiths (Table 1) and imply that reorganisation of crustal heat production occurred on the terrane scale. Assuming that the complement of the HPE now in the upper crustal granites was recycled from the deeper crust, McLaren & Sandiford (2001) calculated that the HPE redistribution associated with all granite generation in the Mount Isa Block would have equated to long-term cooling of the deep crust of *c.* 200 °C.

QUANTITATIVE CONSIDERATIONS

The discussion in the previous section highlights the fact that individual granite complexes, such as the Sybella Batholith, may host a significant proportion of the crustal HPE complement. The segregation of these melts from their source regions is therefore associated with a significant differentiation of the HPEs. In this section we provide an assessment of the thermal effects of granite generation, which explicitly addresses the consequences of HPE redistribution. We begin by considering the long-term thermal consequences of this redistribution by comparing the steady-state conductive thermal regime following granite emplacement with the thermal regime appropriate to the HPE distribution prior to granite generation. We then consider the time dependent effect of the conductive

Table 1. Selected average heat production values for major Australian Proterozoic granite suites within the Central Shield Province.

Terrane	Granite Type	Age range	Area of outcrop (km^2)	% area of outcrop	U (p.p.m)	Th (p.p.m)	K (wt%)	H (μWm^{-3})
Mount Isa	Williams & Naraku	1490–1545	1883	5	13.5	55.5	3.90	**10.13**
	Sybella	1660	1231	3	7.1	37.6	5.26	**6.93**
	Rift-related*	1620–1790	4323	11	6.6	33.5	5.60	**6.59**
	Kalkadoon	1800–1860	4686	12	5.3	25.6	4.71	**5.41**
	All granites		**10935**	**27**				
Pine Creek	Burnside	1750–1800	300	0.6	11.1	38.1	4.85	**8.65**
	Cullen	1810–1890	8325	17	7.3	31.9	4.53	**6.69**
	All granites		**8626**	**18**				
Arunta Inlier	Mount Webb	<1400	6155	4	9.8	43.0	4.52	**7.78**
	Southwark	1680–1560	6720	4	4.1	30.0	3.77	**4.67**
	Jervois-Jinka	1820–1710	12587	8	8.4	48.4	4.96	**8.41**
	All granites		**27233**	**18**				
Tennant Creek	Warrego	1670–1720	443	2	8.7	36.4	5.23	**7.51**
	Tennant Creek	1830–1870	2195	10	5.5	23.4	4.60	**5.19**
	All granites		**4131**	**18**				
Kimberley	Sally Downs	1780–1830	2592	5	3.6	19.0	3.46	**3.84**
	Paperbark	1845–1860	9415	6	5.2	20.6	4.48	**4.94**
	Sophie Downs	*c.* 1910	64	1	2.2	16.9	3.66	**3.26**
	All granites		**12073**	**22**				
TOTAL			100477		6.8	32.1	4.62	6.30 #

Note: The average Proterozoic granite heat production values are calculated at 1700 Ma, based on modern day abundances of the heat producing elements. Average U, Th and K data summarized from Wyborn *et al.* (1998). Granites listed in each terrane are major granite suites (loosely grouped using age data and supersuite terminology from Wyborn *et al.*, 1998). This table does not include all granites known from each terrane.

The Kimberley terrane includes both the Halls Creek and King Leopold Orogens.

TOTAL values are determined from an average of all available analyses (and include analyses from terranes not included in the summary compilation above). % area occupied by each major granite group is an estimate based on the accurate outcrop area of the granite, and an estimated area of the entire inlier. Estimates of total inlier area are likely to overestimate the area of outcrop, so the values shown here are likely to be a minimum estimate of the percentage of granite vs. total outcrop.

*the Rift related granites at Mt Isa include the Sybella Batholith.

response to HPE redistribution together with the transient effects of magmatic heat transfer on resulting thermal regimes in these regions. To assess the thermal consequences of granite emplacement we assume a large granite complex with HPE concentrations loosely modelled on the Sybella Batholith from Mount Isa (Table 1). The granite is assumed to acquire its HPE complement either by melting of a deep crustal source, z_s, or by new additions to the lithosphere, and transfers them to the upper crust at the depth of intrusion, z_i. No HPEs are removed from the upper crust as a result of the intrusion. The horizontal dimension of the HPE source is considered to be a variable. We use a finite element algorithm to compute the temperature field on a domain as illustrated in Fig. 5(a). In Fig. 6, solutions are shown for a cartesian domain appropriate to granite complexes with large horizontal aspect ratios (such as the Sybella Batholith), as well as for a cylindrical domain, appropriate to complexes that are close to equidimensional in horizontal section. We note that for the Sybella granite the intrusion depth was probably around 15 km (M. Rubenach, pers. comm. 2000), while the source region was lower crustal (Wyborn *et al.*, 1988) which we assume was at about 35 km depth; implying an ascent distance for the melt of *c.* 20 km. Parameters used in the calculations are listed in Table 2.

Steady-state considerations

The simple 1-D model outlined in the introduction was based on a scenario in which the HPE complement of the granite was introduced into the crust at the time of granite generation, without corresponding lower crustal depletion. In order to model the conductive thermal effects of a confined intrusion of a HPE-rich granite effectively, we assume a heat production anomaly of the form (Fig. 5a):

$$H_{anom}(x,z) = H_i \exp\left(\frac{-(z-z_i)^2}{h_z^2}\right) * \exp\left(\frac{-x^2}{h_x^2}\right) \qquad (3)$$

where z_i is the depth of the locus of the HPE anomaly, H_i is the heat production maximum at the locus of

Table 2. Parameters used in text and figures, with default values applying to calculations unless otherwise stated.

Symbol	Description	Default value
k	Thermal conductivity	2.5 $Wm^{-1}K^{-1}$
q_m	Basal heat flow	20 mWm^{-2}
$q_{background}$	Heat flow contribution of background crustal sources	45 mWm^{-2}
h	Vertical length-scale for background heat production	15 km
q_{anom}	Maximum effective heat flow contribution of anomalous heat sources	20 mWm^{-2}
T_{anom}	Anomalous component of the temperature field, due to anomalous HPE	
T'_{anom}	Maximum temperature anomaly	
ΔT	Long-term change in the temperature field due to the redistribution of HPE. ΔT is a function of z.	
H_s	Background surface heat production (q_{anom}/h)	3 μWm^{-3}
H_i	Anomalous heat production at $z=z_i$, $x=0$	
z_i	Locus of heat production anomaly at $x=0$	15 km
h_x	Half width of heat production anomaly	25 km
h_z	Half-thickness of heat production anomaly	2 km
hs_x	Half width of heat production source region	
h'_x	Ratio of source region half width to half width of anomaly	
z_c	Thickness of crust	
z_s	Locus of source heat production anomaly at $x=0$	35 km

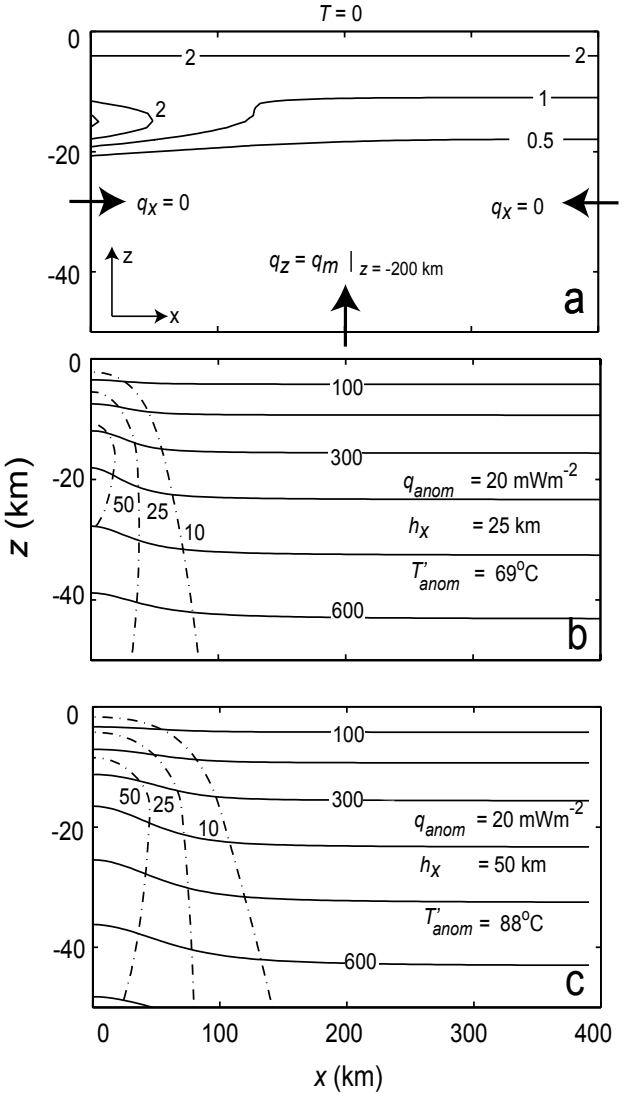

Fig. 5. (a) Computational geometry used in calculation of the thermal consequences of HPE redistribution (only upper 50 km of the 400 by 200 km domain shown). Contours represent the anomalous heat production, $H_{anom}(x, z)$ (b) Temperature field resulting from the heat production anomaly shown in Fig. 5(a) where $h_x = 25$ km, and $q_{anom} = 20$ mWm^{-2}. (c) Temperature field for a heat production anomaly that is twice the width shown in (a), i.e. for $h_x = 50$ km. The dashed lines show the anomalous component of the temperature field, T_{anom} (see Figs 6 & 7).

the anomaly (i.e. at $z=z_i$ and $x=0$) and h_z and h_x provide a measure of the spread of the heat production distribution in the vertical and horizontal directions, respectively (and therefore can be considered as proxies for the half-thickness and half width of the intrusion). The anomaly is superposed on a background heat production field given by the familiar exponential relation of Lachenbruch (1968, 1970):

$$H_{background}(x,z) = H_z \exp\left(\frac{-z}{h_r}\right) \tag{4}$$

such that

$$H(x,z) = H_{anom}(x,z) + H_{background}(x,z) \tag{5}$$

Assuming thermal conductivity is independent of temperature, the steady-state temperature field is given by the solution of the parabolic equation

$$K \cdot \nabla T = -H(x,z) \tag{6}$$

Subject to the boundary conditions shown in Fig. 5(a) (i.e. constant basal heat flux at $z=200$ km and zero horizontal heat flux at $x=0$ and $x=400$ km). Note that these boundary conditions are more geologically reasonable than the simple 1-D formulation given in the introductory section of this paper. We also note that for the parameters listed in Table 2 the solution to the above equations is within 4 °C of the solution for a distribution in which heat production of H_i is confined to a sill of dimension 2 h_z by 2 h_x centred at depth z_i and $x=0$.

We characterise the HPE complement carried by the granite as the vertically integrated anomalous heat production at $x=0$:

$$q_{anom} = \frac{H_i h_z \sqrt{\pi}}{2}\left(\mathrm{Erf}\left(\frac{z_c - z_i}{h_z}\right) + \mathrm{Erf}\left(\frac{z_i}{h_z}\right)\right) \approx H_i h_z \sqrt{\pi} \tag{7}$$

Figure 5(b) shows the temperature field expected from the heat production anomaly shown in Fig. 5(a), with $q_{anom}=20$ mWm^{-2}. Figure 5(c) shows the temperature field for an anomaly that is twice the width of that shown in Fig. 5(a). Note that because the anomalous component of the temperature field, T_{anom}, is linear in the anomalous heat production and conductivity terms, the solution also varies linearly in q_{anom} (Fig. 6), and with the linear inverse of the thermal conductivity. Figure 7 shows the maximum temperature anomaly, T'_{anom}, as a function of geologically plausible variations in q_{anom}, h_x and z_i. For $q_{anom}=20$ mWm^{-2} and $h_x=25$ km the perturbation in the temperature field at $z=-15$ km and $x=0$ is about 70 °C (Figs 5–7). The temperature perturbation drops to less than 1/e of this value at two half widths (i.e. 50 km) and is insignificant at four half widths (e.g. Fig. 5b). The maximum temperature anomaly occurs at depths close to the locus of the heat production anomaly (i.e. z_i). At deeper levels the

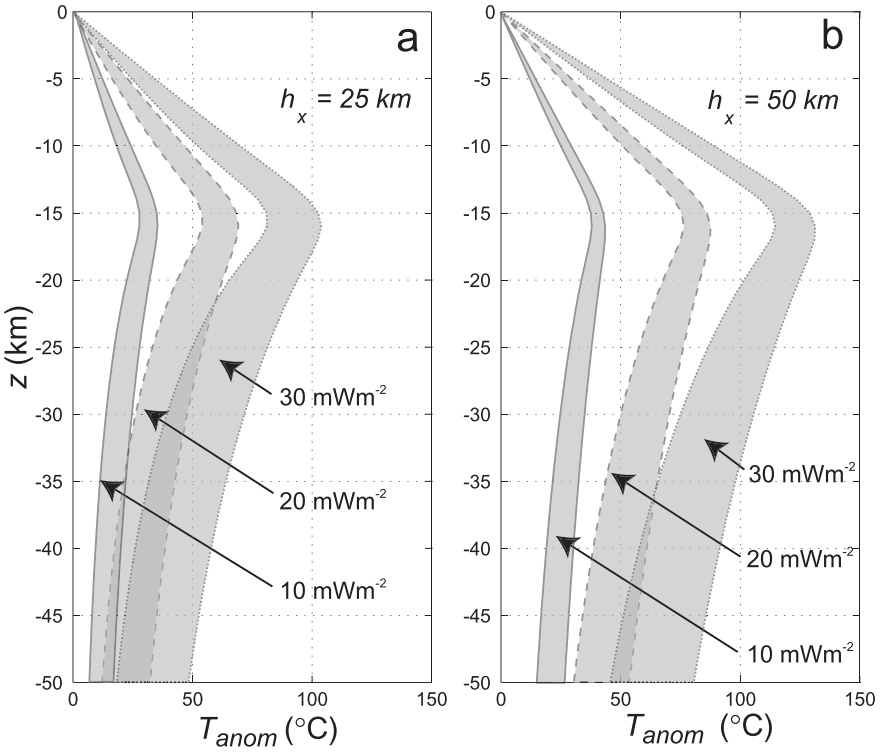

Fig. 6. The magnitude of the anomalous component of the temperature field (T_{anom}) at $x=0$ for (a) $h_x=25$ km and (b) $h_x=50$ km, for a range in q_{anom} equal to 10, 20 and 30 mWm^{-2}, respectively. The thermal anomaly is obtained by subtracting the temperature field due to $H_{background}(x, z)$ from the temperature field due to $H_{anom}(x, z)+H_{background}(x, z)$. Because the solution is linear in the anomalous heat production and conductivity terms, the temperature anomaly increases linearly with q_{anom} and with the linear inverse of the thermal conductivity. The upper and lower bounds on the individual fields represent solutions in a cartesian domain and a cylindrical domain, respectively. The former applies when the horizontal aspect ratio of the granite complex is large, while the latter applies when the complex is equidimensional in horizontal section.

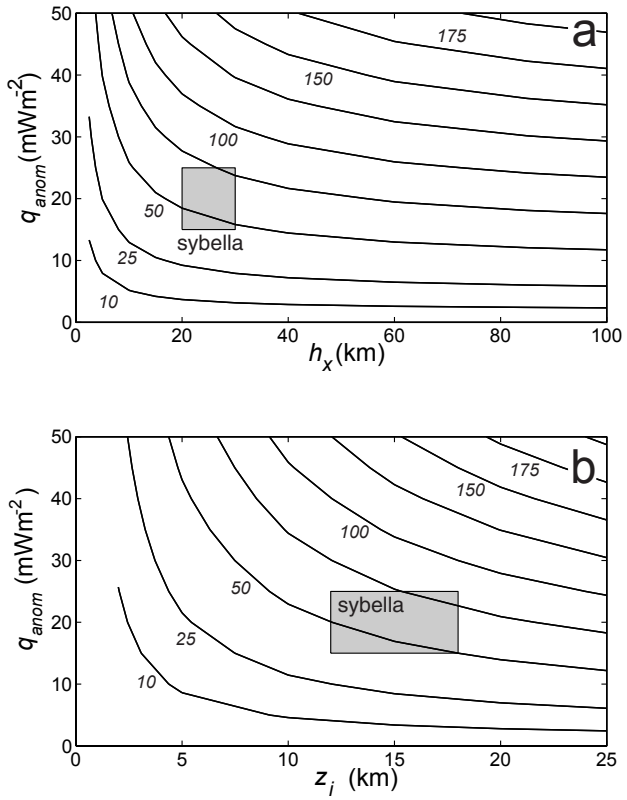

Fig. 7. Dependence of maximum value of the anomalous temperature field (T'_{anom}) on the parameters (a) q_{anom} and h_x, and (b) q_{anom} and z_i. The shaded box shows the likely parameter range for the Sybella Batholith. Solutions are shown for the cartesian domain only.

anomaly declines because lateral heat transfer from beneath the anomalous heat production zone helps to disperse the build-up of heat originating from heat flow through the deeper lithosphere. Nevertheless, for the anomalies modelled here, which are based on large-scale granitic complexes, significant thermal anomalies extend throughout the lower crust and upper mantle (Figs 5 & 6).

The perturbations to the temperature field considered above are relative to a background thermal regime dictated by $H(x, z) = H_{background}(x, z)$. In effect, we have modelled the effect of spontaneously generating the anomalous heat production field. As noted above, this is appropriate only if the HPE complement carried by the granite was introduced into the lithosphere at the time of granite emplacement. However, in view of the lithophile nature of the HPEs it is more likely that the anomalous concentrations carried by the granite were scavenged from deeper crustal levels in the source regions of the granite. In this case it is more appropriate to consider the change in the temperature field relative to the heat source distribution prior to granite generation. To do this we consider a source-region heat production distribution similar to that used to approximate the granite, i.e.

$$H_{source}(x,z) = Hs_i \exp\left(\frac{-(z-z_s)^2}{hs_z^2}\right) * \exp\left(\frac{-x^2}{hs_x^2}\right) \quad (8)$$

The default value of z_s, the locus of the source heat production anomaly, used here represents the case where the HPEs are entirely derived from the crust. Moreover, for the case when the entire HPE complement hosted by the granite is generated from the source region we require (for the Cartesian domain):

$$\int\int H_{anom}(x,z)dxdz = \int\int H_{source}(x,z)dxdz \quad (9)$$

We make no explicit assumptions about the width of the source region from which the HPEs are scavenged. Rather, we consider the ratio of source width to intrusion width as an independent parameter designated h'_x.

To illustrate the thermal consequences of HPE redistribution from source to emplacement level we compare the difference in the steady-state conductive temperature field after granite generation with that prior to granite generation. This long-term change is termed ΔT. Figure 8 shows ΔT for a range in the parameters h_x and h'_x mapped onto the x-z plane. Figure 9 shows ΔT as function of distance from the centre of the intrusion for a range in h'_x. Figure 10 shows ΔT as function of depth for a range in h'_x. For $h'_x = 1$ (i.e. when the width of source anomaly, hs_x, is the same as the intrusion h_x) the redistribution of HPEs results in significant long-term cooling at source levels and minor heating at emplacement levels. For a Sybella-like granite the long-term cooling of the source region is estimated at *c.* 60 °C, while the resulting heating at the intrusion levels is *c.* 20 °C (Fig. 8a). Increasing the parameter h'_x tends to diminish the cooling effect at source regions and augment the heating at intrusion levels. The case of $h'_x = \infty$ corresponds to an infinitely dilute source, as would apply if the complement of HPE contained within the granite represented new additions to the lithosphere. For this case, the long-term temperature changes equate with the temperature field due to $H_{anom}(x, z)$ (i.e. Figs 5–7).

Transient effects

The long-term temperature changes due to the redistribution of HPEs occur over timescales appropriate to the conductive response of the lithosphere. On shorter timescales the temperature field will include thermal transients resulting from (1) readjustment to the new HPE distribution, and (2) the effects of magmatic heat transfer. There will also be additional transient thermal effects associated with any additional heat

source responsible for the melting of the source region. Although this is a significant problem in its own right and is not dealt with rigorously here, it is likely to affect the rate of lower crustal cooling and therefore impact on any attendant phenomena, such as the rate and amount of thermal sag and the formation of associated sedimentary basins (see Discussion). We do not consider such effects in our models and so the transient effects referred to in this section, and in the following Discussion Section, reflect only the component due to

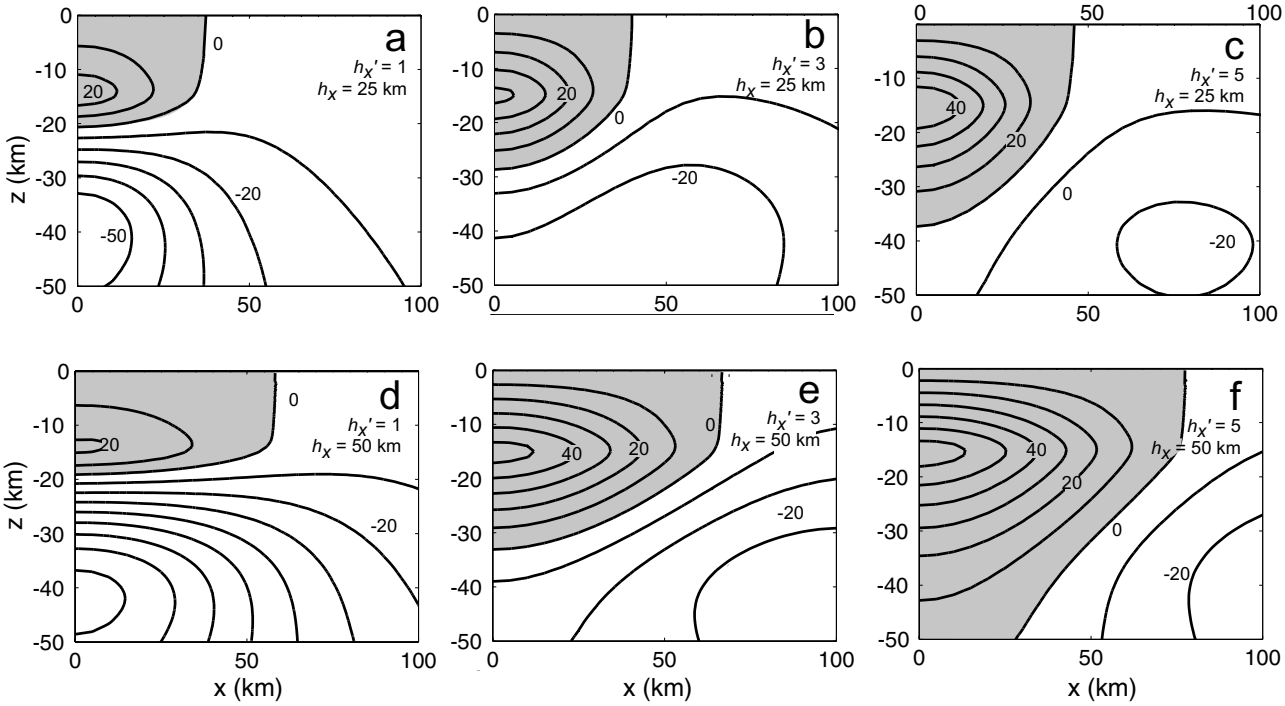

Fig. 8. Predicted long-term changes (ΔT) in the temperature field associated with granite-aided transfer of HPEs from a source region to emplacement level for parameters listed in Table 2. The parameter h_x' is the ratio of effective width of the source region to the width of the intrusion. (a) to (c) are for $h_x = 25$ km, while (d) to (f) are for $h_x = 50$ km (details are shown in Figs 9 & 10). Solutions are shown for the cartesian domain only.

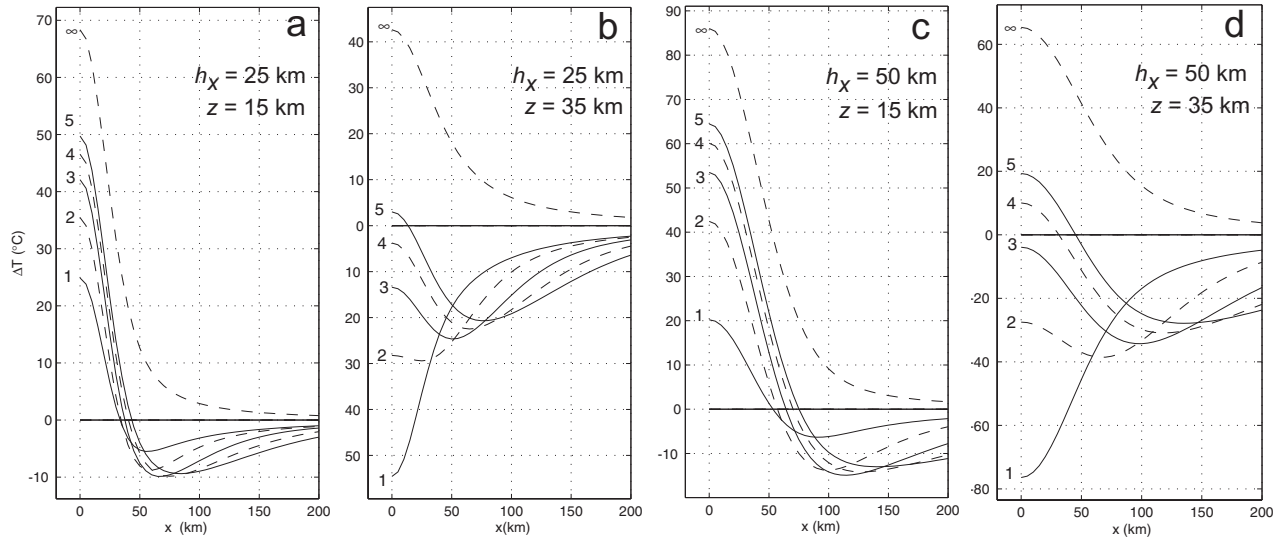

Fig. 9. Variation in long-term temperature changes (ΔT) with horizontal distance from $X = 0$ at the depth of intrusion (a and c) and the depth of the source (b and d). ΔT variations are shown for $h_x' = 1$, 2, 3, 4, 5 & 8. Solutions are shown for the cartesian domain only.

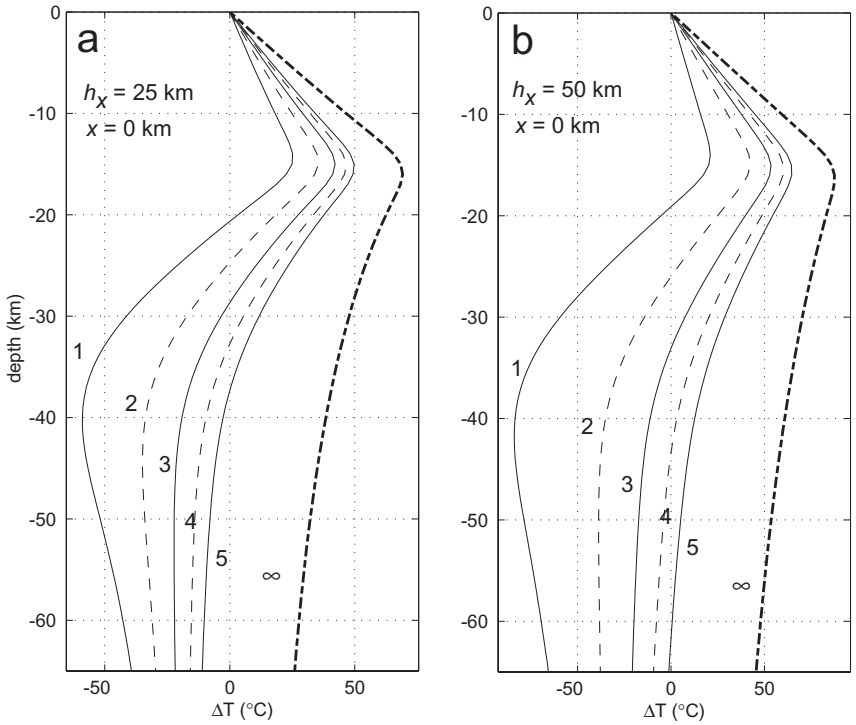

Fig. 10. Variation in long-term temperature changes (ΔT) with depth (z) at $x=0$. ΔT variations are shown for $h'_x=1$, 2, 3, 4, 5 & ∞. Solutions are shown for the cartesian domain only.

the redistribution of HPEs and the advection of heat during granite emplacement.

Figure 11(a,b) shows the timescales appropriate for conductive readjustment to the new HPE distribution, ignoring the effects of advective heat transfer and the latent heat of crystallization. Of particular interest is the thermal response at mid-upper crustal levels (e.g. Fig. 11a), not so much because it provides an accurate portrayal of the likely thermal evolution but rather because it effectively illustrates the competition between the changes in the source and emplacement level heat production distribution. The temperature–time evolution is characterised by an initial phase of heating lasting about 10 Myr followed by cooling towards the steady state lasting around 150 Myr. The initial heating reflects the almost instantaneous impact of the heat production at the site of emplacement, which dominates the early signal at crustal levels in the vicinity of z_i. The removal of heat production from the source region takes *c.* 10 Myr to make a significant impact at these upper crustal levels, by which time these levels have already been heated beyond their ultimate steady-state temperature. In contrast, lower crustal levels experience cooling at all times following extraction of the HPEs from the source region.

The transfer of granite magma from source to emplacement level results in transient thermal perturbations of several hundreds of degrees in the immediate vicinity of the intrusion. Consequently, the amplitude of the magmatic heating-cooling cycle will be much greater than that due to HPE redistribution alone. Figure 11(c,d) shows the predicted thermal evolution for an assumed intrusion temperature of 900 °C. The solid curves incorporate HPE redistribution, and can be compared with the dashed lines, which show the predicted thermal evolution ignoring HPE redistribution. Figure 11(c,d) shows that the temperature-time paths associated with the 'contact aureole' around a HPE-rich granite will be quantitatively affected by the redistribution of HPEs. In particular, HPE redistribution tends to diminish bulk cooling rates in the upper crust and (as implicit in the preceding discussion) change the final, steady-state target to which temperature-time trajectories converge.

DISCUSSION

Since granites are enriched in HPEs relative to bulk crust, the generation and segregation of granites plays an important role in modulating the long-term thermal structure of the lithosphere. Using parameters appropriate to large granitic complexes in Australian Proterozoic terranes, our calculations show that the transfer of HPEs from the source regions to emplacement levels can induce long-term changes in temperature of the order of 50 °C. Source regions are characterised by long-term cooling, while emplacement levels are characterised by long-term heating. In detail, the predicted thermal changes are sensitive to the amount and transport distance of the HPEs, and the extent to which the granitic HPE complement is scavenged from lithospheric sources.

Recognising that the generation of large-scale granitic complexes leads to long-term changes in

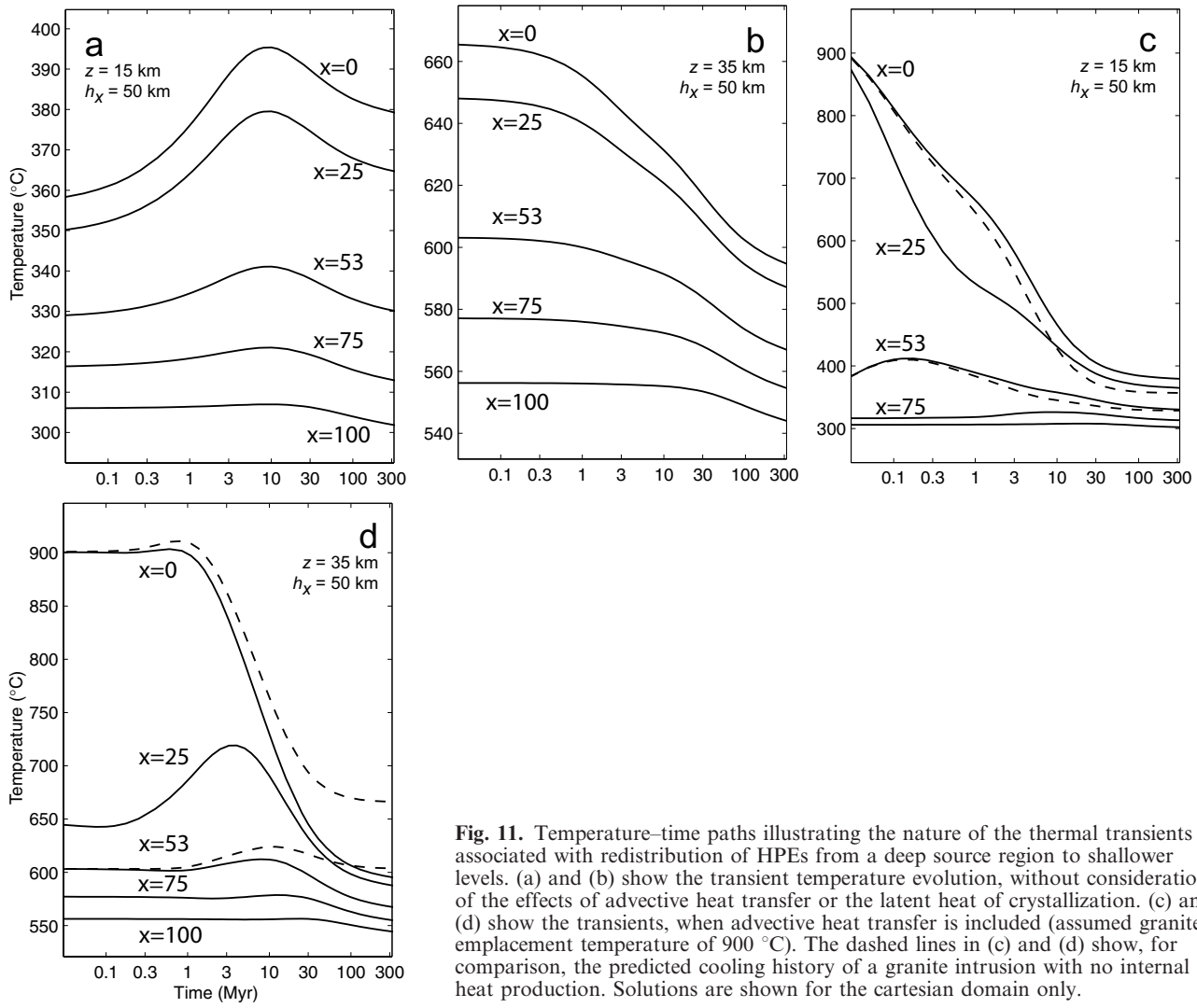

Fig. 11. Temperature–time paths illustrating the nature of the thermal transients associated with redistribution of HPEs from a deep source region to shallower levels. (a) and (b) show the transient temperature evolution, without consideration of the effects of advective heat transfer or the latent heat of crystallization. (c) and (d) show the transients, when advective heat transfer is included (assumed granite emplacement temperature of 900 °C). The dashed lines in (c) and (d) show, for comparison, the predicted cooling history of a granite intrusion with no internal heat production. Solutions are shown for the cartesian domain only.

lithospheric thermal regime raises the question of the role of granitic magmatism in stabilising continental lithosphere. Because the mechanical strength of lithosphere is sensitive to its thermal regime (e.g. Sonder & England, 1986), HPE redistribution associated with the development of large granitic complexes will affect the long-term strength of the lithosphere. In particular, cooling of the upper mantle by as much as 50 °C due to the transport of HPEs from source regions to emplacement levels will be associated with very significant lithospheric strengthening. The differentiation of HPEs into the upper crust through large-scale granite magmatism is therefore likely to be essential for the development of continental lithosphere that is sufficiently strong to act in a cratonic fashion. While these ideas are not inherently new, the calculations summarised in this paper provide a quantitative estimate of the thermal changes associated with granite generation and provide a basis for investigating the associated changes in mechanical properties of the lithosphere (see Sandiford & McLaren, 2001).

As we have shown, the generation of large-scale, HPE-rich granitic complexes may lead to significant, long-term deep crustal and upper mantle cooling. The associated increase in density of the lithosphere will have the isostatic consequence of inducing subsidence, in an entirely analogous fashion to the thermal sag that follows lithospheric extension. In order to show this effect we have calculated the isostatic subsidence that follows from the development of a granitic complex, modelled on the Sybella Batholith, as illustrated in Fig. 8. For the case where the accommodation space created by the subsidence is entirely filled with sediment (with an assumed density of 2500 kg^{-3}) the resulting basin may attain thicknesses approaching 1 km (Fig. 12). In the case of Mount Isa, rift-related granites

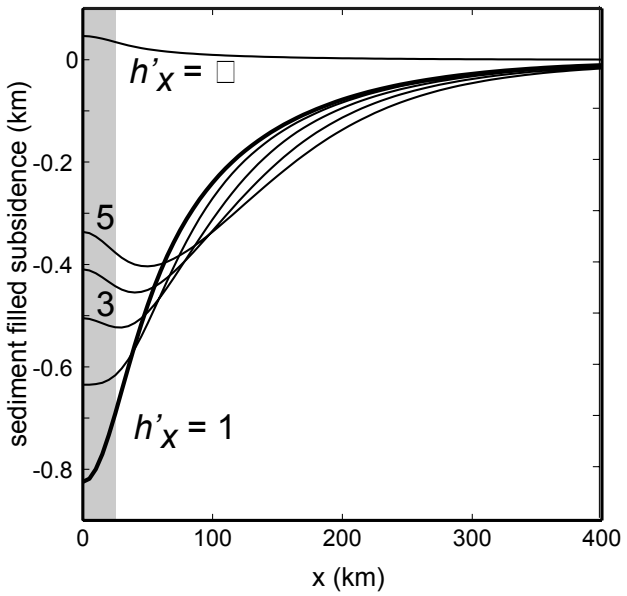

Fig. 12. Estimates of the thermal subsidence associated with the long-term temperature changes following HPE redistribution in a Sybella — like granite complex. The subsidence is calculated assuming local isostatic balance, and that the accommodation space created by the subsidence is entirely filled with sediment of density 2500 kg^{-3}.

such as the Sybella Batholith do indeed precede an extended phase of thermal subsidence, during which thick sedimentary sequences were deposited. As illustrated in Fig. 12, at least part of this subsidence may be attributed to the thermal consequences of the redistribution of HPEs associated with generation and segregation of the Sybella Batholith.

ACKNOWLEDGEMENTS

L. Wyborn and I. Bastrakova are thanked for access to and assistance with the Australian Geological Survey Organization Granite GIS dataset, used in the generation of Table 1. We are grateful to N. Mancktelow and R. A. Jamieson for their helpful, constructive reviews of the manuscript.

REFERENCES

Chapman, D. S. & Furlong, K. P., 1977. Continental heat flow-age relationships. *EOS, Transactions of the American Geophysical Union*, **58,** 1240.

Collins, C. D. N., 1991. The nature of the crust–mantle boundary under Australia from seismic evidence. *Geological Society of Australia Special Publications* (ed. B. J. Drummond), **17,** 67–80.

Connors, K. A. & Page, R. W., 1995. Relationships between magmatism and deformation in the western Mount Isa Inlier, Australia. *Precambrian Research*, **71,** 131–153.

Cull, J. P., 1982. An appraisal of Australian heat-flow data. *Bureau of Mineral Resources Journal of Australian Geology and Geophysics*, **7,** 11–21.

Fowler, C. M. R., 1990. *The Solid Earth: an Introduction to Global Geophysics*. Cambridge University Press, New York.

Haenel, R., Rybach, L. & Stegena, L., eds. 1988. *Handbook of Terrestrial Heat-flow Density Determination; With Guidelines and Recommendations of the International Heat Flow Commission*, Kluwer, Dordrecht.

Lachenbruch, A. H., 1968. Preliminary geothermal model of the Sierra Nevada. *Journal of Geophysical Research*, **73,** 6977–6989.

Lachenbruch, A. H., 1970. Crustal temperature and heat production: implications of the linear heat flow relation. *Journal of Geophysical Research*, **75,** 3291–3300.

McCready, T., 1997. Geologic interpretation of the Mount Isa deep seismic transect. PhD Thesis, *Monash University, Melbourne*.

McLaren, S. & Sandiford, M., 2001. Long-term thermal consequences of tectonic activity at Mount Isa, Australia: Implications for polyphase tectonism in the Proterozoic. In: *Polyphase Tectonism and Reactivation Mechanisms in Metamorphic Belts, Geological Society of London. Special Publications 184* (eds Miller, J. A., Holdsworth, R. G., Buick, I. S. & Hand, M.), 219–236, Geological Society, London.

McLaren, S., Sandiford, M. & Hand, M., 1999. High radiogenic heat producing granites and metamorphism — an example from the western Mount Isa Inlier, Australia. *Geology*, **27,** 679–682.

McLennan, S. M. & Taylor, S. R., 1996. Heat flow and the chemical composition of continental crust. *Journal of Geology*, **104,** 369–377.

Morgan, P., 1984. The thermal structure and thermal evolution of the continental lithosphere. In: Pollack, H. N. & Murthy, V. R., eds. Structure and evolution of the continental lithosphere. *Physics and Chemistry of the Earth*, **15,** p. 107–185.

Neumann, N., Sandiford, M. & Foden, J., 2000. Regional geochemistry and continental heat flow: Implications for the origin of the South Australian heat flow anomaly. *Earth and Planetary Science Letters*, **183,** 107–120.

Pollack, H. N., Hurter, S. J. & Johnson, J. R., 1993. Heat flow from the Earth's interior: Analysis of the global heat flow dataset. *Review of Geophysics*, **31,** 267–280.

Sandiford, M. & Hand, M., 1998. Controls on the locus of Phanerozoic intraplate deformation in central Australia. *Earth and Planetary Science Letters*, **162,** 97–110.

Sandiford, M., Hand, M. & McLaren, S., 1998. High geothermal gradient metamorphism during thermal subsidence. *Earth and Planetary Science Letters*, **163,** 149–165.

Sandiford, M. & McLaren, S., 2002. Thermo-mechanical controls on heat production distributions and the long-term evolution of the continents. In: *'Evolution and Differentiation of the Continental Crust'* (eds Brown, M. & Rushmer, T.), Cambridge University Press, Cambridge.

Sass, J. H. & Lachenbruch, A. H., 1979. Thermal regime of the Australian continental crust. In: *The Earth — Its Origin, Structure and Evolution* (ed. McElhinny, M. W.), pp. 301–351. Academic Press, London.

Sonder, L. & England, P. C., 1986. Vertical averages of rheology of the continental lithospheric; relation to thin sheet parameters. *Earth and Planetary Science Letters*, **77,** 81–90.

Van der Hilst, R. D., Kennett, B. L. N., Christie, D. & Grant, L., 1994. SKIPPY mobile broad-band arrays to study the seismic structure of the lithosphere and mantle beneath Australia. *EOS, Transaxrions of the American Geophysical Union*, **75,** 177–181.

Wyborn, L. A. I., Budd, A. R. & Bastrakova, I. V., 1998. The metallogenic potential of Australian Proterozoic granites, Granite GIS (Partial Release) CD ROM, Australian Geological Survey Organization, Canberra.

Wyborn, L. A. I., Page, R. W. & McCulloch, M. T., 1988. Petrology, geochronology and isotope geochemistry of the post-1820 Ma granites of the Mount Isa Inlier; mechanisms

for the generation of Proterozoic anorogenic granites. *Precambrian Research*, **41,** 509–541.

Wyborn, L. A. I., Wyborn, D., Warren, R. G. & Drummond, B. J., 1992. Proterozoic granite types in Australia: implications for lower crust composition, structure and evolution. *Transactions of the Royal Society of Edinburgh Earth Sciences*, **83,** 201–209.

Zielhaus, A. & Van der Hilst, R. D., 1996. Upper-mantle shear velocity beneath eastern Australia from inversion of waveforms from SKIPPY portable arrays. *Geophysical Journal International*, **127,** 1–16.

Received 14 November 2000; revision accepted 28 March 2001